

## OZITX, a pertussis toxin-like protein for occluding inhibitory G protein signalling including $G\alpha_z$

Alastair C. Keen <sup>1,2,3,13</sup>, Maria Hauge Pedersen<sup>4,5,6,13</sup>, Laura Lemel<sup>2,3</sup>, Daniel J. Scott <sup>7,8</sup>, Meritxell Canals<sup>2,3</sup>, Dene R. Littler<sup>9</sup>, Travis Beddoe <sup>10</sup>, Yuki Ono<sup>11</sup>, Lei Shi<sup>12</sup>, Asuka Inoue <sup>11</sup>, Jonathan A. Javitch <sup>4,5,14</sup>✉ & J. Robert Lane <sup>2,3,14</sup>✉

Heterotrimeric G proteins are the main signalling effectors for G protein-coupled receptors. Understanding the distinct functions of different G proteins is key to understanding how their signalling modulates physiological responses. Pertussis toxin, a bacterial AB<sub>5</sub> toxin, inhibits  $G\alpha_{i/o}$  G proteins and has proven useful for interrogating inhibitory G protein signalling. Pertussis toxin, however, does not inhibit one member of the inhibitory G protein family,  $G\alpha_z$ . The role of  $G\alpha_z$  signalling has been neglected largely due to a lack of inhibitors. Recently, the identification of another Pertussis-like AB<sub>5</sub> toxin was described. Here we show that this toxin, that we call OZITX, specifically inhibits  $G\alpha_{i/o}$  and  $G\alpha_z$  G proteins and that expression of the catalytic S1 subunit is sufficient for this inhibition. We identify mutations that render  $G\alpha$  subunits insensitive to the toxin that, in combination with the toxin, can be used to interrogate the signalling of each inhibitory  $G\alpha$  G protein.

<sup>1</sup> Drug Discovery Biology, Monash Institute of Pharmaceutical Sciences, Monash University, Parkville, VIC 3052, Australia. <sup>2</sup> Division of Physiology, Pharmacology and Neuroscience, School of Life Sciences, Queen's Medical Centre, University of Nottingham, Nottingham, UK. <sup>3</sup> Centre of Membrane Proteins and Receptors, University of Birmingham and University of Nottingham, Nottingham, UK. <sup>4</sup> Departments of Psychiatry and Molecular Pharmacology and Therapeutics, Vagelos College of Physicians and Surgeons, Columbia University, New York, NY, USA. <sup>5</sup> Division of Molecular Therapeutics, New York State Psychiatric Institute, New York, NY, USA. <sup>6</sup> NNF Center for Basic Metabolic Research, Section for Metabolic Receptology, Faculty of Health and Medical Sciences, University of Copenhagen, Copenhagen, Denmark. <sup>7</sup> Department of Biochemistry and Molecular Biology, University of Melbourne, Parkville, VIC 3052, Australia. <sup>8</sup> The Florey Institute of Neuroscience and Mental Health, University of Melbourne, Parkville 3052 VIC 3052, Australia. <sup>9</sup> Infection and Immunity Program and Department of Biochemistry and Molecular Biology, Biomedicine Discovery Institute, Monash University, Clayton, VIC 3052, Australia. <sup>10</sup> Department of Animal, Plant and Soil Science and Centre for AgriBioscience, La Trobe University, Bundoora, VIC 3086, Australia. <sup>11</sup> Graduate School of Pharmaceutical Sciences, Tohoku University, Sendai, Miyagi 980-8578, Japan. <sup>12</sup> Computational Chemistry and Molecular Biophysics Section, National Institute on Drug Abuse - Intramural Research Program, National Institutes of Health, Baltimore, MD, USA. <sup>13</sup> These authors contributed equally: Alastair C. Keen, Maria Hauge Pedersen. <sup>14</sup> These authors jointly supervised this work: Jonathan A. Javitch, J. Robert Lane. ✉email: [Jonathan.Javitch@nyspi.columbia.edu](mailto:Jonathan.Javitch@nyspi.columbia.edu); [rob.lane@nottingham.ac.uk](mailto:rob.lane@nottingham.ac.uk)

Heterotrimeric guanine nucleotide-binding proteins (G proteins) are important signalling transducers that link cell-surface receptors such as G protein-coupled receptors (GPCRs) to intracellular effectors<sup>1–3</sup>. They consist of a G $\alpha$  subunit as well as G $\beta$  and G $\gamma$  subunits that function as an obligate dimer. There are four subfamilies of G $\alpha$  subunits (G $\alpha_s$ , G $\alpha_i$ , G $\alpha_q$  and G $\alpha_{12}$ ) based on sequence similarity. Their functions can be broadly generalised based on this classification. The stimulatory (G $\alpha_s$ ) and the inhibitory (G $\alpha_i$ ) subfamilies stimulate and inhibit adenylate cyclases, respectively<sup>1,4</sup>. The G $\alpha_q$  subfamily activates phospholipase C- $\beta$  leading to increases in cytosolic Ca<sup>2+</sup>, and the G $\alpha_{12}$  subfamily activates Rho family GTPases that regulate cytoskeletal processes<sup>2,5</sup>. Understanding the distinct signalling roles of individual members of each subfamily is central to our comprehension of how they control different physiological processes.

The G $\alpha$  subunit, and in particular its carboxy tail, is largely responsible for determining the specificity of the interaction with an activated GPCR<sup>6,7</sup>. The GPCR acts as a guanine nucleotide exchange factor, promoting the exchange of bound GDP for GTP at the guanine nucleotide-binding domain of the G $\alpha$  subunit. This causes the G $\alpha$  subunit to dissociate from, or rearrange relative to, the G $\beta\gamma$  dimer, and both then act on downstream effectors<sup>8,9</sup>. The G $\alpha$  subunit is a GTPase, hydrolysing GTP to restore GDP to the binding domain, allowing the G $\beta\gamma$  dimer to reassociate and completing the cycle.

AB<sub>5</sub>-type toxins have proved to be useful tools for the interrogation of G protein signalling. These toxins are characterised by a hetero-hexameric structure consisting of the enzymatically active A subunit and pentameric ring of B subunits, which are responsible for recognition of host cell-surface receptors and facilitate cellular entry. In order to modulate host cell behaviour, AB<sub>5</sub> toxins have varied actions on their targets, including protease activity<sup>10</sup>, RNA N-glycosidase activity<sup>11</sup> and ADP-ribosylation<sup>12</sup>. Of relevance to G-protein signalling, cholera toxin acts on the G $\alpha_s$  subfamily<sup>13</sup> and *Pasteurella multocida Pasteurella multocida* toxin acts on the G $\alpha_i$ , G $\alpha_q$  and G $\alpha_{12}$  family to render them constitutively active<sup>14</sup>. Pertussis toxin (PTX), from *Bordetella pertussis*, ADP ribosylates all members of the G $\alpha_i$  subfamily, except for G $\alpha_z$ <sup>15</sup>. Researchers have exploited these actions to identify the G $\alpha$  subunits responsible for particular cell signalling processes. PTX-driven ADP ribosylation occurs on a cysteine residue of four residues from the carboxy terminus of G $\alpha_i$  subunits, rendering them incapable of coupling to GPCRs. PTX-insensitive G $\alpha_{i/o}$  subunit mutants, in which the cysteine modified by PTX is replaced by another residue, have been used to understand the role of individual G $\alpha_i$ -subfamily members in vitro. One inhibitory G-protein family member, G $\alpha_z$ , lacks this cysteine and is thus insensitive to PTX. G $\alpha_z$  has a slow GDP-GTP exchange rate, slow GTP hydrolysis rate, and a restricted pattern of expression<sup>16–19</sup>. Despite these unique characteristics, relatively little is known about the physiological role of G $\alpha_z$  signalling, although evidence has been provided for its roles in circadian behaviours, dopaminergic signalling, and pancreatic islet  $\beta$  cell biology<sup>19–22</sup>. Its function in other physiological processes remains elusive, in part due to its insensitivity to PTX. Indeed, there may be cases in which inhibitory G protein signalling has been ruled out based on a lack of PTX effect while neglecting the potential role of G $\alpha_z$ .

A recent publication reported the identification and structural characterisation of a PTX-like protein derived from a uropathogenic *Escherichia coli*<sup>23</sup>. The toxin has an active A subunit homologous to that of PTX and has a similar overall structural fold (Supplementary Fig. 1). Application of this toxin to HEK 293 cells, African green monkey kidney cells or bovine brain lysate revealed its substrates as heterotrimeric G proteins<sup>23</sup>. Using G $\alpha_{12}$

as a substrate in vitro, the toxin was shown to have distinct site(s) of ADP ribosylation from that of PTX—an asparagine residue and a lysine residue eight and ten residues from the carboxy terminus, respectively<sup>23</sup>. The asparagine is conserved across several G $\alpha$  subunits, suggesting that the toxin may have broader substrate specificity than PTX.

In this study, we show that this toxin inhibits the coupling of all G $\alpha_{i/o/z}$  G proteins, including G $\alpha_z$ . Thus, we refer to it as G $\alpha_o$ , G $\alpha_z$  and G $\alpha_i$  inhibiting ToXin, or in short; OZITX. The active A subunit is functional when expressed in mammalian cells, bypassing the need for toxin purification. Moreover, we generate mutants of the members of the G $\alpha_i$  subfamily that are OZITX insensitive, and hence, can serve as tools in combination with OZITX treatment to investigate the role of individual G $\alpha_{i/o/z}$  G proteins.

## Results

**OZITX treatment abolishes GPCR-mediated activation of all G $\alpha_i$  subfamily members, including G $\alpha_z$ .** We hypothesised that OZITX may display a broader selectivity as compared to PTX because the Asn<sup>348</sup> residue that is ADP ribosylated by OZITX is conserved in a greater number of G $\alpha$  subunits as opposed to the cysteine modified by PTX, which is only present in G $\alpha_i$  and G $\alpha_o$  family members (Fig. 1a, b)<sup>23</sup>. We first sought to determine whether OZITX inhibits coupling to members of the inhibitory G protein subfamily. To achieve this, we used a previously described bioluminescence resonance energy transfer (BRET) assay that measures the release of G $\beta\gamma$  subunits from the G $\alpha$  subunits upon activation of the heterotrimer (Fig. 2a)<sup>24,25</sup>. While this assay provides a method for rapidly assessing G protein activation, the signal may be partially contaminated by endogenously expressed G $\alpha$  subunits<sup>25,26</sup>. We, therefore, adapted the assay for use in HEK293A CRISPR/Cas  $\Delta$ G $\alpha$ -all cells in which all the G $\alpha$  subunits had been genetically knocked out<sup>27</sup>. This allowed us to monitor the G $\beta\gamma$  release specifically from the activation of one G $\alpha$  subtype of interest that had been exogenously transfected.

The dopamine D<sub>2</sub> receptor (D<sub>2</sub>R) promiscuously couples to G $\alpha_{i/o}$  and G $\alpha_z$  G proteins<sup>28,29</sup>. Cells transiently expressing the D<sub>2</sub>R were pre-incubated with PTX or OZITX followed by stimulation with the D<sub>2</sub>-like receptor-selective agonist ropinirole<sup>30</sup>. We observed that OZITX completely blocked the activation of G $\alpha_{i1}$ , G $\alpha_{i2}$ , G $\alpha_{i3}$ , G $\alpha_{oA}$  and G $\alpha_{oB}$  (Fig. 2b). Further, as predicted from the carboxy-tail Asn<sup>348</sup> residue presented in G $\alpha_z$ , G $\alpha_z$  could no longer couple to the D<sub>2</sub>R following OZITX treatment as well (Fig. 2b). In contrast, G $\alpha_z$  was insensitive to inhibition by pre-treatment of cells with PTX, consistent with the absence of the required cysteine residue (Fig. 1a). This finding extends the initial characterisation of OZITX, showing that unlike PTX it can inhibit G $\alpha_z$  as well as G $\alpha_{i/o}$ <sup>23</sup>.

Next, analogous experiments were performed with another G $\alpha_{i/o/z}$ -coupled GPCR; the  $\mu$  opioid receptor. HEK293A CRISPR/Cas  $\Delta$ G $\alpha$  cells transiently expressing the MOPR were pre-incubated with either OZITX or PTX and then stimulated with the agonist DAMGO (Fig. 2c). OZITX inhibited coupling to each of the G $\alpha_{i/o/z}$  subunits completely (Fig. 2c). This showed, as expected, that OZITX does not discriminate between GPCRs when inhibiting G $\alpha_{i/o/z}$  G-protein activation.

We then sought to further characterise the toxin by measuring the activation of G $\alpha_{12}$  by the D<sub>2</sub>R after exposure to OZITX at different timepoints. G $\alpha_{12}$  activation decreased with increasing time of OZITX exposure until G $\alpha_{12}$  activation was completely abolished approximately sixteen hours after the addition of OZITX (Fig. 2d). This is consistent with the characteristics of PTX and suggests that OZITX, like PTX, would be best utilised in the laboratory by incubating with the cells for more than 16 h (Supplementary Fig. 2).

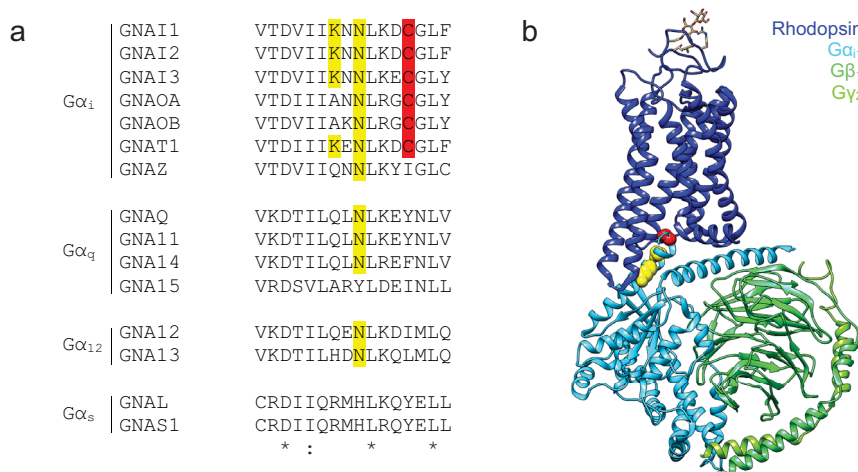


**Fig. 1 Identification of G $\alpha$  carboxy-tail amino acid residues that are putatively ADP-ribosylated by OZITX.** **a** Amino acid sequence alignment of carboxy-terminal residues of heterotrimeric G $\alpha$  proteins. Sequences were aligned with Clustal Omega version 1.2.4. ‘\*’ represents a completely conserved residue. ‘.’ represents a conserved residue (>0.5 in the Gonnet PAM 250 matrix). ‘.’ represents a weakly conserved residue ( $\leq 0.5$  and >0 in the Gonnet PAM 250 matrix). Cysteine residues ADP-ribosylated by PTX are indicated in red. Putative lysine and asparagine residues ADP-ribosylated by OZITX identified by Littler and colleagues<sup>23</sup> are indicated in yellow. The asparagine residue that is a putative substrate is conserved across many G $\alpha$  subunits. **b** The location of OZTX’s and PTX’s substrate amino acid sites within a GPCR-G protein complex. The structure of rhodopsin bound to G $\alpha_{i1}\beta_1\gamma_2$  is depicted in the cartoon (PDB code 6CMO). Rhodopsin is shown in dark blue, G $\alpha_{i1}$  in light blue, G $\beta_1$  in green and G $\gamma_2$  in light green. The carboxy-terminal Cys<sup>351</sup> residue ADP-ribosylated by PTX is shown in red spheres. Lys<sup>345</sup> and Asn<sup>347</sup>, the putative residues ADP-ribosylated by OZITX, are highlighted in yellow spheres. Graphic constructed using UCSF chimera.

### OZITX does not ablate G $\alpha_s$ , G $\alpha_q$ or G $\alpha_{12}$ subfamily coupling.

In addition to the inhibitory G $\alpha$  G protein subfamily, the asparagine eight residues from the carboxy terminus is conserved in other G $\alpha$  subfamily members (Fig. 1a). We therefore sought to further assess the substrate selectivity of OZITX across all G $\alpha$  subunits. The G $\alpha_s$  subfamily possesses a histidine residue instead of an asparagine in this position. In accordance with OZITX’s proposed mechanism of action, overnight incubation with OZITX did not inhibit G $\alpha_s$  or G $\alpha_{olf}$  activation by the dopamine D<sub>1</sub> receptor, a G $\alpha_{s/olf}$ -coupled receptor, stimulated with the D<sub>1</sub>R-selective agonist SKF83822 (Fig. 3a)<sup>31–34</sup>.

G $\alpha_q$ , G $\alpha_{11}$  and G $\alpha_{14}$ , but not G $\alpha_{15}$ , possess an asparagine residue eight residues from their C termini, so one might expect these three subunits to be substrates for OZITX (Fig. 1a). We measured the activation of the G $\alpha_q$  subfamily proteins by the G $\alpha_q$ -coupled neurotensin receptor 1 stimulated by the agonist NT8-13 with and without OZITX treatment<sup>35,36</sup>. OZITX pre-treatment did not inhibit the activation of G $\alpha_q$ , G $\alpha_{11}$  or G $\alpha_{15}$  although G $\alpha_{14}$  activation was slightly (~25%) decreased (vehicle control = 0.0840, OZITX-treated = 0.0644,  $P = 0.0012$ , one-way ANOVA with Dunnett’s multiple comparisons test) (Fig. 3b).

Both members of the G $\alpha_{12}$  subfamily; G $\alpha_{12}$  and G $\alpha_{13}$ , also have asparagine as their eighth to last residue (Fig. 1a). The neurotensin receptor 1 is known to couple to the G $\alpha_{12}$  subfamily<sup>37</sup>. While we were successful in detecting robust activation of G $\alpha_{12}$  and G $\alpha_{13}$ , there was no inhibitory effect on the activation of either subunit when the cells were treated with OZITX (Fig. 3c). Taken together, we conclude that despite the presence of this asparagine residue at the C-terminus of G $\alpha_q$  and G $\alpha_{12}$  subfamily members, no detectable inhibitory action of OZITX was observed, with the exception of the limited inhibition of G $\alpha_{14}$ .

**Inhibition of cAMP production by G $\alpha_{i2}$ -, G $\alpha_{oA}$ - and G $\alpha_z$  is inhibited by OZITX.** Cell-surface receptor signalling is commonly amplified in subsequent steps down the signalling cascade. We wanted to confirm that the apparent complete blockade of G $\alpha_{i/o/z}$  signalling at the level of G-protein coupling would concord with measurements further downstream. We assessed the

effect of OZITX treatment in measurements of intracellular cAMP levels using an intramolecular conformational BRET sensor of cAMP (CAMYEL), since the G $\alpha_i$  subfamily bind and inhibit adenylate cyclases<sup>4,38</sup>. In these experiments, we used HEK293A cells that harbour a genetic knockout of all the G $\alpha_i$  subfamily members using CRISPR/Cas (HEK293A CRISPR/Cas  $\Delta$ G $\alpha_i$ )<sup>27</sup>. Individual G $\alpha_i$  subunits of interest were then transfected into this cell background. Cells were treated with forskolin to stimulate adenylate cyclase, followed by treatment with ropinirole to stimulate the D<sub>2</sub>R, leading to activation of the G $\alpha_{i/o/z}$  subunit of interest. In the absence of a transfected G $\alpha$  subunit, there was no detectable drug-induced inhibition of cAMP production (Fig. 4a). When G $\alpha_{i2}$  or G $\alpha_{oA}$  were transfected, activation of the D<sub>2</sub>R produced a decrease in relative cAMP levels (indicated by an increase in BRET ratio) and this was completely abolished in cells treated with OZITX (Fig. 4b, c). Cells transfected with G $\alpha_z$  also produced a decrease in cAMP, albeit to a slightly smaller degree, and this was again blocked in the presence of OZITX (Fig. 4d). This confirms that OZITX-mediated ADP-ribosylation inhibits downstream G $\alpha_{i/o/z}$ -mediated signalling.

### The active A subunit of OZITX can be transfected into mammalian cells to act as an inhibitor.

In order to treat cells with AB<sub>5</sub> toxin protein complexes, both expression and purification of this toxin are required<sup>23</sup>. The active A subunit of PTX alone can be transiently expressed to inhibit G $\alpha_{i/o}$  signalling<sup>39,40</sup>. Accordingly, we tested whether the OZITX would be functional upon transfection of the cDNA encoding the active A subunit alone (OZITX-S1), thus increasing its accessibility and utility to laboratories. The cDNA sequence of OZITX-S1 was codon-optimised for high expression in human cells and co-transfected into HEK293T cells along with the D<sub>2</sub>R, the WT G $\alpha_{i/o/z}$  subunits and the G-protein activation sensors. Upon activation of the D<sub>2</sub>R with the agonist quinpirole the responses in cells transfected with G $\alpha_{i1-3}$ , G $\alpha_{oA}$  and G $\alpha_{oB}$  were inhibited in cells transfected with the positive control PTX-S1 cDNA as well as the OZITX-S1 cDNA (Fig. 5a–c and Supplementary Fig. 3). Importantly, while transfection of cells with OZITX-S1 inhibited G $\alpha_z$  activation,

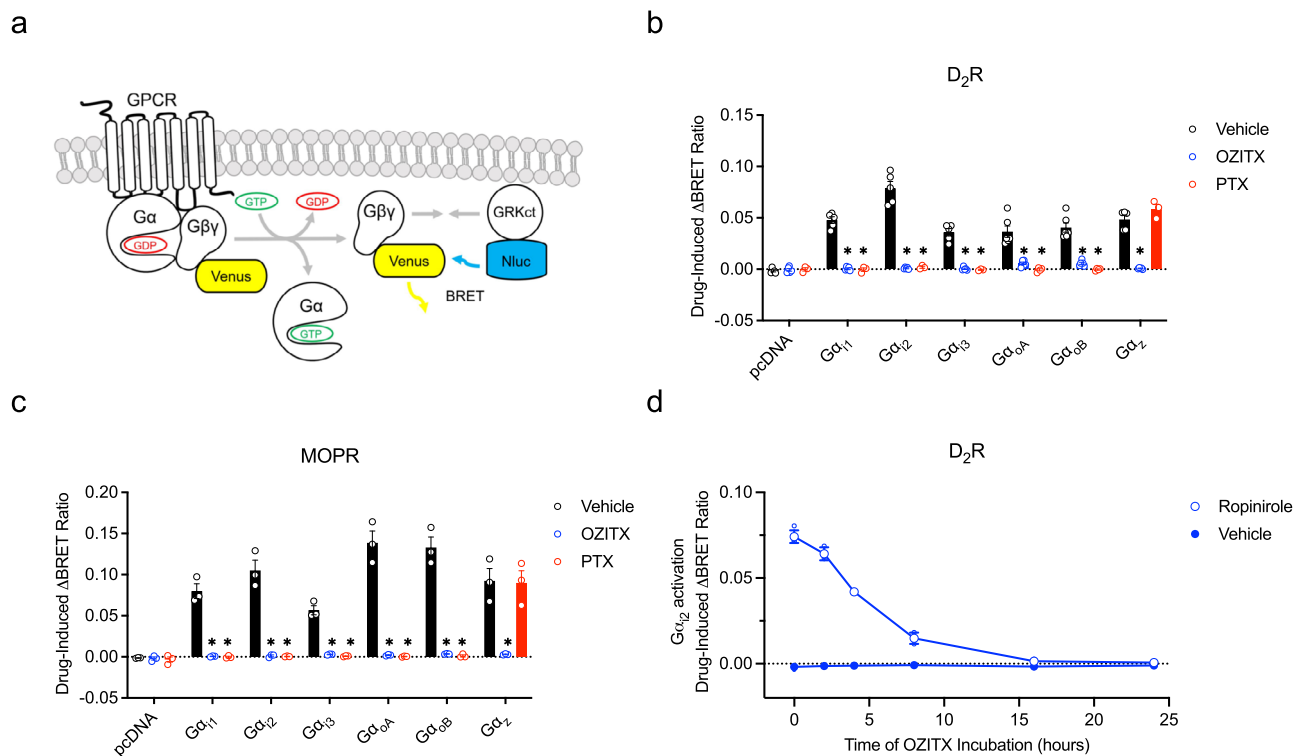


**Fig. 2** Activation of members of the  $G\alpha_i$  subfamily in the presence of OZITX and PTX. **a** Representation of the BRET sensors used for detection of G-protein activation. The  $G\alpha\beta\gamma$  heterotrimer is activated through agonist binding to the GPCR and the  $G\alpha$  and  $G\beta\gamma$ -venus dissociate. Free  $G\beta\gamma$ -venus is bound by masGRK3ct-Nluc that serves as a BRET donor resulting in non-radiative energy transfer from Nluc to venus. **b** Dopamine  $D_2$ receptor ( $D_2R$ )-mediated activation or **(c)**  $\mu$  opioid receptor (MOPR)-mediated activation of  $G\alpha_i$  subfamily members in the presence of OZITX or PTX. HEK293A CRISPR/Cas  $\Delta G\alpha$ -all cells expressing the  $D_2R$  or MOPR were pre-treated with either vehicle (black), OZITX (blue) or PTX (red) for 24 h. Cells were stimulated with  $1\ \mu\text{M}$  ropinirole ( $D_2R$ ) or  $1\ \mu\text{M}$  DAMGO (MOPR) for 2.5 min followed by BRET detection. Data represent the mean drug-induced increase in BRET ratio from vehicle  $\pm$  SEM from six independent experiments ( $D_2R$ ) or three independent experiments (MOPR). \*Represents where the response is significantly different ( $P < 0.001$ ) from the respective vehicle toxin untreated control condition (black bar) as determined by a one-way ANOVA with Dunnett's multiple comparisons test. **d** Time course of OZITX treatment on G-protein activation. HEK 293  $\Delta G\alpha$ -all cells were transfected with cDNA encoding the  $D_{2L}R$ ,  $G\alpha_{12}$  and G-protein activation sensors. Cells were pre-treated with OZITX for the indicated times. BRET was measured 2.5 min after stimulation with  $1\ \mu\text{M}$  ropinirole (blue open circles) or vehicle (blue filled circles). The basal BRET ratio prior to agonist stimulation has been subtracted to give the drug-induced  $\Delta$ BRET ratio. Data represent the mean  $\pm$  SD from three separate experiments. Individual replicates are shown as small circles.

transfection of PTX-S1 cDNA did not. Having shown that transfected OZITX-S1 is functional, we then confirmed the pattern of OZITX selectivity across the  $G\alpha$  subfamilies was in accord with our previous results using treatment with the complete OZITX protein complex (Supplementary Fig. 3). Consistent with these findings, the OZITX-S1 transfection was ineffective in abolishing the activation of  $G\alpha_s$ ,  $G\alpha_q$  and  $G\alpha_{12}$  subfamilies (Supplementary Fig. 3). In contrast to the partial inhibition of  $G\alpha_{14}$  that we observed when using the purified OZITX (Fig. 3b), we did not observe inhibition of  $G\alpha_{14}$  in experiments transiently expressing the OZITX-S1 (Supplementary Fig. 3).

ADP ribosylation of the C-terminal cysteine of  $G\alpha_{i/o}$  subunits by PTX is thought to inhibit the functional interaction between these G proteins and an activated GPCR. To test whether ADP ribosylation might also inhibit such an interaction we measured the recruitment of  $G\alpha_{oA}:G\beta\gamma$ -venus G protein heterotrimers to the  $D_{2L}R$  in the presence of either PTX-S1 or OZITX-S1 expression. Our data clearly show that both PTX and OZITX inhibit  $G\alpha_{oA}:G\beta\gamma$ -venus G-protein heterotrimer recruitment to the  $D_2R$  but that only OZITX inhibits  $G\alpha_z:G\beta\gamma$ -venus G-protein heterotrimer recruitment, as expected. This is consistent with a mechanism of action whereby ADP ribosylation of the C-terminal asparagine of  $G\alpha_{i/o/z}$  by OZITX prevents their coupling to GPCRs akin to the action of PTX at the C-terminal cysteine of  $G\alpha_{i/o}$  (Supplementary Fig. 4).

**$G\alpha_i$  subunits can be made OZITX insensitive for dissection of  $G\alpha_{i/o/z}$  subtype signalling specificity.** Understanding the actions of a single  $G\alpha_{i/o/z}$  subtype can be challenging because there are usually multiple  $G\alpha_{i/o/z}$  members expressed within any given cell type. A method that has permitted the investigation of the role of individual  $G\alpha_{i/o/z}$  subunits in a particular signalling process, such as coupling to a specific GPCR, is the use of PTX-insensitive  $G\alpha_i$  mutants in combination with PTX to uncouple any endogenously expressed PTX-sensitive  $G\alpha_i$  subunits<sup>41</sup>. We, therefore, wanted to generate OZITX-insensitive  $G\alpha_{i/o/z}$  mutants in the hope of increasing the scope of OZITX applications. To render the  $G\alpha_{i/o/z}$  subunits insensitive to OZITX, we replaced the asparagine eight residues from the carboxy terminus to an alanine ( $G\alpha_{11}$ -N347A,  $G\alpha_{12}$ -N348A,  $G\alpha_{13}$ -N347A,  $G\alpha_{oA}$ -N347A,  $G\alpha_{oB}$ -N347A and  $G\alpha_z$ -N348A) as this residue was previously identified as the most likely substrate site (Fig. 1a)<sup>23</sup>. We then performed G protein-activation assays using the  $D_2R$  to activate each  $G\alpha_i$  mutant in the presence or absence of PTX-S1 or OZITX-S1 (Fig. 5 and Supplementary Figs. 5 and 6). In contrast to the activation of the wild-type  $G\alpha_{13}$ ,  $G\alpha_{oA}$  and  $G\alpha_z$  that are all abolished by OZITX (Fig. 5a–c), activation of  $G\alpha_{13}$ -N347A,  $G\alpha_{oA}$ -N347A and  $G\alpha_z$ -N348A were OZITX insensitive (Fig. 5d–f). When these mutant  $G\alpha$  subunits were transfected the potency of quinpirole was similar to that observed in the case of the WT  $G\alpha$  subunit, suggesting that these mutations did not affect the efficiency with which they couple to

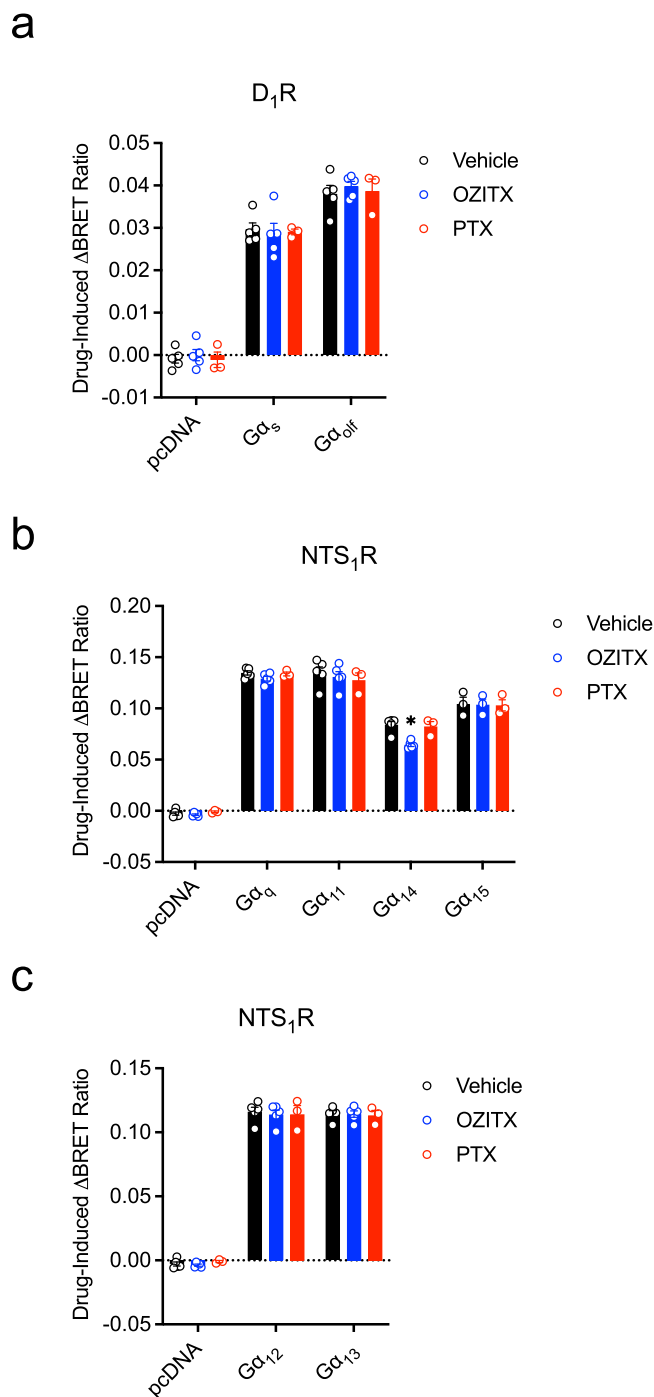


**Fig. 3** G $\alpha$ <sub>s</sub>, G $\alpha$ <sub>q</sub> and G $\alpha$ <sub>12</sub> subfamily activation in presence of OZITX and PTX. **a** Activation of G $\alpha$ <sub>s</sub> subfamily members by the dopamine D<sub>1</sub> receptor (D<sub>1</sub>R) in the presence of OZITX and PTX. **b** Activation of G $\alpha$ <sub>q</sub> subfamily members by NTS<sub>1</sub>R in the presence of OZITX and PTX. **c** Activation of G $\alpha$ <sub>12</sub> subfamily members by the neurotensin receptor 1 (NTS<sub>1</sub>R) in the presence of OZITX and PTX. HEK 293 ΔGα-all CRISPR cells were transfected with cDNA encoding the particular GPCR and G $\alpha$  together with the G-protein activation sensors as described in “Methods”. The cells were pre-treated with either vehicle (black), OZITX (blue) or PTX (red) for 24 h before stimulation with the agonists 100 nM SKF83822 (D<sub>1</sub>R)/1 μM NT8-13 (NTS<sub>1</sub>R) for 2.5 min followed by BRET detection. The data are represented as the mean drug-induced increase in BRET ratio from vehicle control ± SEM from three separate experiments. \*Represents where the OZITX or PTX-treated condition is significantly different ( $P < 0.001$ ) from the vehicle-treated condition (black) as determined by a one-way ANOVA with Dunnett’s multiple comparisons test.

the D<sub>2</sub>R. In addition, it was observed that the N347A/N348A mutation did not impact the PTX sensitivity of the G $\alpha$ <sub>i</sub> subunits (Fig. 5d–f). Likewise, the well-characterised PTX-insensitive mutation (C351I) introduced into G $\alpha$ <sub>i3</sub> and G $\alpha$ <sub>oA</sub>, did not disturb the ability of OZITX to act on them (Fig. 5g, h). Having identified that the N347A/N348A mutation renders these G $\alpha$ <sub>i</sub> members insensitive to OZITX without perturbation, the mutations were extended into the remaining G $\alpha$ <sub>i</sub> subunits and validated (Supplementary Figs. 5 and 6).

**The C-terminal ten residues of G $\alpha$ <sub>i</sub> are sufficient to confer OZITX selectivity.** The asparagine residue important for the inhibitory action of OZITX is present in both the G $\alpha$ <sub>i/o/z</sub> and the G $\alpha$ <sub>q</sub> subfamilies (with the exception of G $\alpha$ <sub>15</sub>). Thus, the selective action of OZITX at the G $\alpha$ <sub>i/o/z</sub> G-protein  $\alpha$  subunits appears not to be determined solely by the presence or absence of this residue. Similarly, a previous study has shown that replacement of the 5 C-terminal residues of G $\alpha$ <sub>q</sub> with that of G $\alpha$ <sub>i</sub> (which includes the cysteine that is modified by PTX) allows this chimeric G $\alpha$ <sub>qi5</sub> G protein to couple to G<sub>i</sub> protein family-coupled receptors but, importantly, does not confer sensitivity to PTX<sup>42</sup>. This suggests that there are determinants of PTX in addition to the presence of this cysteine residue. To explore other determinants of OZITX selectivity we generated two chimeric G proteins in which the last 10 (G $\alpha$ <sub>qi10</sub>) or 13 (G $\alpha$ <sub>qi13</sub>) residues of G $\alpha$ <sub>q</sub> were replaced with those of G $\alpha$ <sub>i3</sub>, a region that includes the asparagine residue modified by OZITX. In an assay measuring Ca<sup>2+</sup> mobilisation, OZITX was unable to inhibit the Ca<sup>2+</sup> response of the muscarinic M<sub>3</sub> acetylcholine receptor co-expressed with G $\alpha$ <sub>q</sub> when activated by the agonist carbachol (Supplementary Fig. 7). In this Ca<sup>2+</sup> mobilisation assay we were unable to detect a measurable response to the agonist ropinirole when the D<sub>2</sub>R was co-expressed with G $\alpha$ <sub>q</sub>, but we observed responses when the D<sub>2</sub>R was co-expressed with both chimeric G proteins, meaning the D<sub>2</sub>R can couple to both G $\alpha$ <sub>qi10</sub> and G $\alpha$ <sub>qi13</sub>. Interestingly, both PTX and OZITX could inhibit these responses, indicating that the last 10 residues of G $\alpha$ <sub>i</sub> are sufficient to confer the sensitivity to both PTX and OZITX inhibition on a G $\alpha$ <sub>q</sub> background (Supplementary Fig. 7). While both PTX and OZITX partially inhibited the G $\alpha$ <sub>qi10</sub> Ca<sup>2+</sup> signal, the expression of both toxins completely inhibited G $\alpha$ <sub>qi13</sub> signalling. This pattern is consistent with the idea that the greater the amount of C-terminal G $\alpha$ <sub>i</sub> amino acids swapped with those of G $\alpha$ <sub>q</sub>, the better the chimeric G $\alpha$ <sub>qi</sub> proteins become as substrates for both  $\alpha\beta_5$  toxins. However, the lower potency of ropinirole in the G $\alpha$ <sub>qi13</sub> Ca<sup>2+</sup> assay suggests that the coupling of the D<sub>2</sub>R to this chimera is less efficient, which may also account for the apparently greater inhibitory effect of PTX and OZITX (Supplementary Fig. 7).

## Discussion

For decades, PTX and CTX have proven to be useful tools in GPCR signalling research to interrogate the G $\alpha$  protein subfamilies or even specific G $\alpha$  proteins responsible for particular physiological processes. Here, we characterise and demonstrate the utility of OZITX, a recently identified AB<sub>5</sub> toxin, for the inhibition of GPCR-mediated activation of the G $\alpha$ <sub>i/o/z</sub> subfamily. Importantly, unlike PTX, this activity extends to include G $\alpha$ <sub>z</sub>. OZITX acts to ADP-ribosylate an asparagine in the C-terminus of G $\alpha$ <sub>i/o/z</sub> proteins, a site distinct from the cysteine modified by PTX, accounting for this broader specificity. We found that OZITX displays a selective action to completely inhibit G $\alpha$ <sub>i/o/z</sub> proteins with no activity at G $\alpha$ <sub>s</sub>, G $\alpha$ <sub>q</sub> or G $\alpha$ <sub>12</sub> proteins, with the exception of limited inhibition of G $\alpha$ <sub>14</sub>. The catalytic subunit of PTX (PTX-S1) can be expressed in mammalian cells to effectively inhibit G $\alpha$ <sub>i/o</sub> signalling, avoiding the time and cost associated with acquiring the purified protein<sup>39,40</sup>. We demonstrate that the catalytic OZITX-S1 subunit can be used in a similar

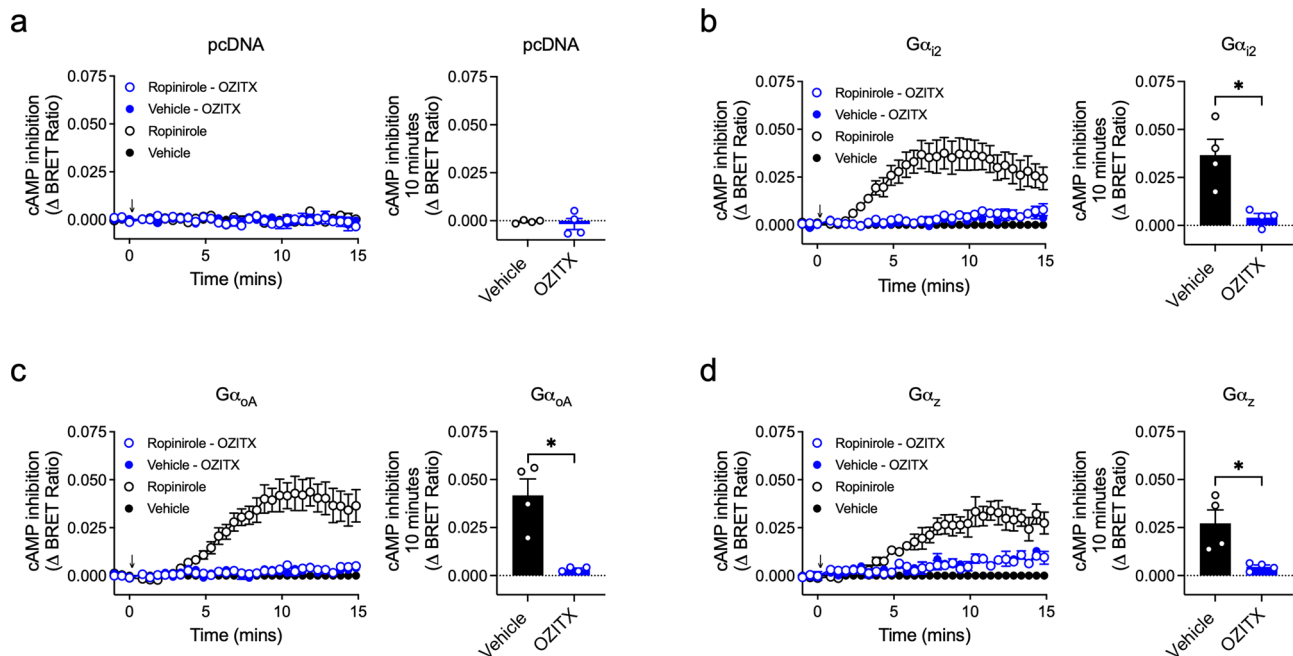


**Fig. 4** The effect of OZITX on  $G\alpha_{i2}$ -,  $G\alpha_{oA}$ - and  $G\alpha_z$ -mediated inhibition of cAMP production. Inhibition of forskolin-stimulated cAMP production was detected in live cells using CAMEL; a conformational BRET sensor based on EPAC. HEK 293  $\Delta G\alpha_{i/o}$  CRISPR cells were transfected with DNA encoding the  $D_2R$ , CAMEL and either (a) pcDNA3.1+ control, (b)  $G\alpha_{i2}$ , (c)  $G\alpha_{oA}$  or (d)  $G\alpha_z$ . Transfected cells were then incubated with either vehicle (black) or OZITX (blue) for 24 h. Cells were then pre-stimulated with 10  $\mu$ M forskolin for 10 min before stimulation with either vehicle control (filled circles) or 1  $\mu$ M ropinirole (open circles). Data are baseline-corrected to the cells not treated with OZITX or ropinirole and is shown as the mean  $\pm$  SEM from four separate experiments. Measurements of cAMP inhibition between vehicle and OZITX-treated conditions were compared using an unpaired Student's *t* test \* represents statistical significance  $P < 0.05$  (pcDNA  $-P = 0.700$ ,  $G\alpha_{i2}$   $-P = 0.008$ ,  $G\alpha_{oA}$   $-P = 0.004$ ,  $G\alpha_z$   $-P = 0.019$ ).

manner, increasing the utility of this tool. We identify mutations within  $G\alpha_{i/o/z}$  subfamily members that render them insensitive to OZITX and maintain their ability to couple to GPCRs. Together, these tools can be used to identify the  $G\alpha_{i/o/z}$  subunits participating in defined signalling pathways.

PTX played an important role in identifying the  $G\alpha_i$  subfamily by distinguishing it from the  $G\alpha_s$  subfamily<sup>4</sup>. PTX was shown to block the inhibitory effect that  $G\alpha_i$  proteins have on adenylyl cyclases, thus building evidence for a separate Ga species with distinct functionality to  $G\alpha_s$ . Since then, PTX has been widely used with the same rationale, that is, to differentiate GPCR responses mediated by  $G\alpha_i$  proteins from other signal transducers<sup>43</sup>. However, such an approach cannot exclude the possibility that  $G\alpha_z$  might contribute to a particular response since it is insensitive to PTX<sup>17,18</sup>. A clear advantage of OZITX, then, is that it can inhibit  $G\alpha_z$  in addition to inhibiting  $G\alpha_{i1}$ ,  $G\alpha_{i2}$ ,  $G\alpha_{i3}$  and the  $G\alpha_o$  isoforms. We have not evaluated whether OZITX inhibits the coupling of the visual and taste Ga subunits;  $G\alpha_{t1}$ ,  $G\alpha_{t2}$  and  $G\alpha_{gust}$ . One might expect ADP ribosylation by OZITX to occur on  $G\alpha_{t1}$ ,  $G\alpha_{t2}$  and  $G\alpha_{gust}$  since they harbour an asparagine as their eighth to last amino acid residue in addition to having high sequence homology to the other  $G\alpha_i$  subunits, although given our findings that not all Ga subunits that contain this asparagine are inhibited by OZITX, inhibitor activity at  $G\alpha_{t1}$ ,  $G\alpha_{t2}$  and  $G\alpha_{gust}$  must be determined experimentally.

Our findings suggest that OZITX could serve as a replacement for PTX in most experimental paradigms aimed at interrogating  $G\alpha_{i/o/z}$  G-protein signalling. There are, however, cases where PTX and OZITX can be used in parallel due to their different Ga specificities, for example when disentangling the functions of  $G\alpha_z$  from the other  $G\alpha_{i/o}$  subunits. OZITX-treated, PTX-treated and -untreated conditions run in parallel would enable the signalling mediated by  $G\alpha_z$ , PTX-sensitive  $G\alpha_i$  subunits and toxin-insensitive Ga subunits to be isolated.

Previous studies aimed at interrogating  $G\alpha_z$  signalling have relied on other strategies, including overexpression of  $G\alpha_z$ -specific RGS proteins<sup>19</sup>,  $G\alpha_z$ -directed siRNA<sup>44</sup>, and  $G\alpha_z$  deactivation via PKC phosphorylation<sup>45</sup>. However, unlike OZITX, these approaches do not completely block activation of  $G\alpha_z$  so the influence of residual  $G\alpha_z$  signalling cannot be excluded, particularly when looking at an effect further down an amplified signalling cascade. Genetic knockouts of the gene that encodes  $G\alpha_z$  have been used for this reason but are technically challenging as compared to OZITX treatment<sup>20,46</sup>. In addition, the results of such knockout approaches may be confounded by adaptive changes to the cell and/or circuit over time that compensate for the loss of that particular protein. The advantage of OZITX is that it can be used in a relatively acute manner following overnight treatment, so its use is less likely to be confounded by compensatory changes in cell function.

The substrate site that is ADP ribosylated by OZITX was shown to be an asparagine eight residues from the C-terminus of the Ga subunit<sup>23</sup>. In agreement with this, we showed that  $G\alpha_i$  subunits can be made OZITX insensitive through mutation of the aligned asparagine in this position. Within our set of experiments, we observed that these mutations did not affect the potency or magnitude of the measured response as compared to when the WT Ga was used. This indicates that this mutation has not changed the coupling efficiency between the receptor and Ga subunit. It should be acknowledged, however, that these observations may be both receptor and downstream effector dependent. It may be that other mutations at this position may be superior to the alanine mutation for a particular combination, as has been observed for analogous studies using PTX and PTX-insensitive Ga mutants<sup>47</sup>. Nonetheless, the OZITX-insensitive mutants can serve as a useful tool in combination with OZITX treatment to investigate the signalling of particular  $G\alpha_{i/o/z}$  proteins in isolation. In our hands, mutation of the Asn<sup>347/348</sup>

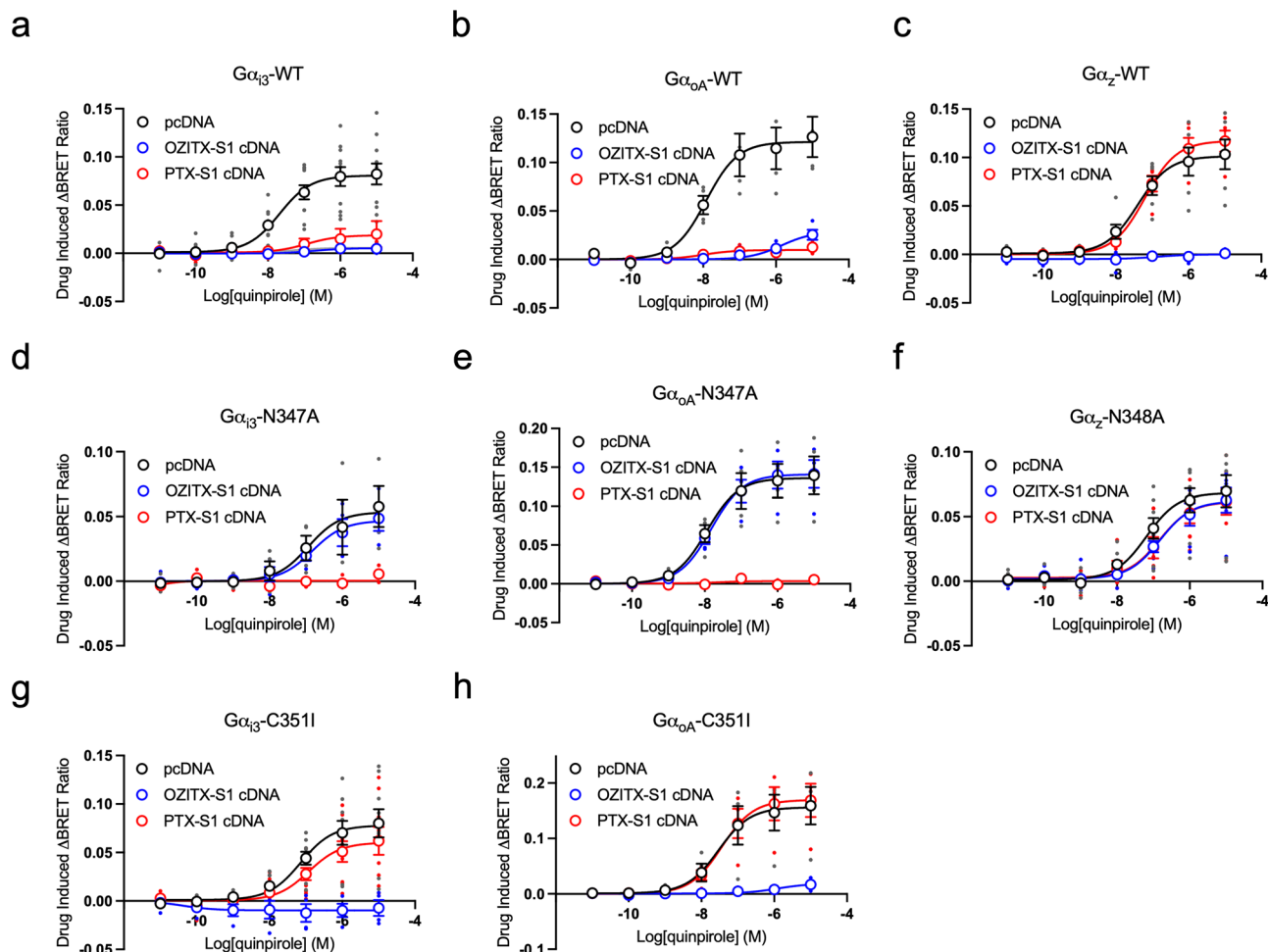


**Fig. 5** OZITX sensitivity of  $G\alpha_i$  subfamily carboxy-tail Asn347/348 mutants. **a**  $G\alpha_{13}$ -WT activation,  $n = 11$ . **b**  $G\alpha_{oA}$ -WT activation,  $n = 4$ . **c**  $G\alpha_z$ -WT activation,  $n = 5$ . **d**  $G\alpha_{13}$ -N347A activation,  $n = 4$ . **e**  $G\alpha_{oA}$ -N347A activation,  $n = 4$ . **f**  $G\alpha_z$ -N347A activation,  $n = 6$ . **g**  $G\alpha_{13}$ -C351 activation,  $n = 4$ . **h**  $G\alpha_{oA}$ -C351 activation,  $n = 4$ . The G-protein activation assay was performed on WT, Asn347Ala/Asn348Ala (putative OZITX site) and Cys351Ile (PTX-insensitive) mutants. Cells were transfected with the  $D_2R$ , the particular  $G\alpha$  mutant, the G-protein activation sensors and either a pcDNA3.1+ control (black open circles), OZITX-S1 cDNA (blue open circles) or PTX-S1 cDNA (red open circles). Cells were then stimulated with increasing concentrations of quinpirole before BRET detection. Data represent the mean drug-induced increase in BRET ratio from vehicle  $\pm$  SEM. Individual replicates are shown as small circles.

residue alone was sufficient to render  $G\alpha_{i1}$ ,  $G\alpha_{i2}$  and  $G\alpha_{i3}$  resistant to OZITX. These  $G\alpha$  subunits contain a lysine residue as their tenth-to-last residue ( $Lys^{345/346}$ ) that was suggested to also be a site for OZITX-mediated ADP ribosylation by Littler and colleagues (Fig. 1a)<sup>23</sup>. Our results suggest that this  $Lys^{345/346}$  site is either a secondary substrate site that is minimally ADP-ribosylated by OZITX, that ADP ribosylation of this site has no effect on G-protein coupling despite this residue being in close proximity to the GPCR upon coupling, or that the ribosylation of this lysine occurs sequentially to that of Asn<sup>347/348</sup> (Fig. 1b), such that the mutation of the asparagine residue is sufficient to abrogate reaction.

We hypothesised that the presence of an asparagine residue eight residues from the C-terminus of various  $G\alpha$  subunits would confer sensitivity to OZITX in a similar manner to the way in which the presence of Cys<sup>351/352</sup> confers sensitivity to PTX. In agreement with this,  $G\alpha_{i/o/z}$  proteins were inhibited by OZITX whereas  $G\alpha_s$ , which lacks this asparagine, was not. We observed, however, that OZITX only had a small inhibitory effect on  $G\alpha_{i4}$  activation and had no effect on the remaining  $G\alpha_q$  and  $G\alpha_{i2}$  subunits despite the presence of the aligned asparagine. Thus, this asparagine is not the only determinant of selectivity. This lack of

OZITX sensitivity can be reconciled either with OZITX not ADP-ribosylating the asparagine residue in  $G_q$  and  $G_{i2}$  family  $G\alpha$  subunits or with ADP ribosylation of this residue in  $G_q$  and  $G_{i2}$  not affecting GPCR coupling and signalling. Prior studies have shown that swapping the five carboxy-terminal residues of  $G\alpha_{i2}$  or  $G\alpha_{oA}$  onto  $G\alpha_q$  is not sufficient to confer sensitivity to PTX, even though the modified  $G\alpha_q$  contains the required cysteine residue four amino acids from the carboxy-termini<sup>42</sup>. This indicates that carrying the required substrate amino acid site is not sufficient to render the  $G\alpha$  subunit sensitive to PTX-like AB<sub>5</sub> toxins. Our own experiments using chimeras in which the last ten or thirteen amino acids of  $G\alpha_q$  were swapped with those of  $G\alpha_{i2}$  revealed that exchange of this region was sufficient to confer both PTX and OZITX sensitivity. We computationally explored the feasibility of ADP-ribosylation of  $G\alpha$  subunits in the  $D_2R$ - $G\alpha_i$  and the  $5HT_{2A}$ - $G\alpha_q$  complexes, by covalently docking the ADP-ribose moiety on the asparagine residue using the available cryo-EM structures of these complexes<sup>48,49</sup>. Our results reveal that the  $5HT_{2A}$ - $G\alpha_q$  complex can easily accommodate the ADP-ribosylated asparagine whereas this covalent docking approach could not identify any feasible pose for the  $D_2R$ - $G\alpha_i$  complex without steric clash (Supplementary Fig. 8). Even though

ADP-ribosylation of the asparagine can be sterically accommodated in the 5HT<sub>2A</sub>-Gα<sub>q</sub> complex, we cannot rule out the possibility that this might still impact coupling, and as we have noted above, the residue may simply not be ADP-ribosylated due to the absence of other key determinants beyond the asparagine itself. Further studies are required to understand the additional structural basis for the recognition of specific Gα subunits by AB<sub>5</sub>-type toxins such as OZITX and PTX and to understand the selective action of OZITX for G<sub>i/o/z</sub> family G proteins.

Our study illustrates the continuing value in the characterisation and use of AB<sub>5</sub> toxins as laboratory tools. Host-pathogen interactions are hotspots of molecular evolution that result in proteins with extraordinary functionality. This is exemplified in the diversity of actions of ADP-ribosylating AB<sub>5</sub> toxins including PTX and CTX and now OZITX and their resulting value as research tools.

## Methods

**Materials.** Polyethyleneimine (PEI), Linear (MW 25,000) was purchased from Polysciences, Inc. Ropinirole was purchased from BetaPharma (Shanghai) Co. Ltd. DAMGO ((D-Ala<sup>2</sup>, N-Me-Phe<sup>4</sup>, Gly-ol<sup>5</sup>)-enkephalin) was purchased from Mimotopes. SKF83822, neurotensin residues 8-13 (NT8-13), (-)-quinpirole hydrochloride (#1061), acetylcholine chloride (#A2661), carbachol (C4382), D-galactose (#G8270) and pertussis toxin (PTX) were purchased from Sigma-Aldrich. Isoproterenol (#1747) and endothelin-1 (#1160) were purchased from Tocris Bioscience (Bristol, UK). Coelenterazine-h was purchased from both NanoLight™ Technology and Dalton research molecules (#50303-86-9). Forskolin was purchased from Cayman Chemicals (#11018). Nano-Glo™ luciferase assay system, containing the furimazine substrate, was purchased from Promega.

**Plasmids.** pcDNA3.1(+) encoding human constructs of long isoform of the dopamine D<sub>2</sub> receptor (D<sub>2</sub>R), μ opioid receptor (MOPR), dopamine D<sub>1</sub> receptor (D<sub>1</sub>R), neurotensin receptor 1 (NTS<sub>1</sub>R), M<sub>1</sub> muscarinic acetylcholine receptor (M<sub>1</sub>R), β<sub>2</sub>-adrenergic receptor (β<sub>2</sub>AR), endothelin A receptor (ETA<sub>1</sub>R), Gα<sub>i1</sub>, Gα<sub>i2</sub>, Gα<sub>i3</sub>, Gα<sub>oA</sub>, Gα<sub>oB</sub>, Gα<sub>z</sub>, Gα<sub>s</sub>, Gα<sub>12</sub>, Gα<sub>13</sub>, Gα<sub>q</sub>, Gα<sub>11</sub>, Gα<sub>14</sub>, Gα<sub>15</sub>-EE, Gα<sub>12</sub> and Gα<sub>13</sub> were from the cDNA Resource Centre (cDNA.org). pcDNA3L-His-CAMYEL was purchased from ATCC (ATCC MBA-277). masGRK3ct-Nluc, masGRK3ct-Rluc8, venus-1-155-Gy2 and venus-156-239-Gβ<sub>1</sub> were from Nevin Lambert, Augusta University. pCAGGS-Ric8A and pCAGGS-Ric8B were from Asuka Inoue, Tohoku University. The active S1 subunit of OZITX (EcPltAB) was codon-optimised, synthesised and inserted into pcDNA3.1+ (see Supplementary Note 1 for sequence). OZITX-resistant mutations were made in Gα<sub>i1</sub>, Gα<sub>i2</sub>, Gα<sub>i3</sub>, Gα<sub>oA</sub>, Gα<sub>oB</sub> and Gα<sub>z</sub> using site-directed mutagenesis. Primer sequences that were used for the mutagenesis can be found in Supplementary Table 1.

OZITX-resistant mutations were made by changing the eighth to last amino acid to an alanine (indicated in red) by using site-directed mutagenesis with the reverse primers used to the right, the alanine mutation change is shown in red and restriction sites chosen in blue (XhoI) or green (XbaI). The constructs were inserted into pcDNA3.1+ with KpnI and XhoI or XbaI as indicated. The two chimeric proteins Gα<sub>q10</sub> and Gα<sub>q13</sub> were generated using the Q5 site-directed mutagenesis kit from NEB. Primer sequences used for the mutagenesis can be found in Supplementary Table 2. PCR products were then treated with the KLD enzyme mix (kinase, ligase and DpnI) provided with the kit and then transform into NEB Turbo *E. coli* competent cells.

**Cell culture.** HEK293T cells were purchased from ATCC (CRL-3216). HEK293A ΔGα-all CRISPR/Cas knockout cells and HEK293A ΔGα<sub>i/o</sub> CRISPR/Cas knockout cells were generated as described<sup>27</sup>. HEK293T cells, HEK293A ΔGα-all cells and HEK293A ΔGα<sub>i/o</sub> cells were cultured in T175 flasks with Dulbecco's Modified Eagle Medium (DMEM) + GlutaMAX™-I (Gibco, Invitrogen, Paisley, UK) with 10% foetal bovine serum (Corning #35-010) and 1% penicillin/streptomycin (Corning #30-002). All Cells were grown in a humidified incubator in 5% CO<sub>2</sub> at 37 °C and sub-cultured at a ratio of 1/10-1/20.

**Transfection.** Briefly, cells were harvested from T175 flasks and plated into six-well Nunc™ tissue culture plates at a density of 500,000 cells per well. The following day, the media was removed and replaced with fresh media and transfected using PEI as the transfection reagent. The corresponding amounts of PEI and DNA were added to the buffer separately before mixing together, incubating for 20 minutes, and then adding dropwise on top of the cells in the fresh media.

For the G-protein-activation assays where the toxin was added exogenously: The HEK293A ΔGα-all CRISPR knockout cells were transfected using PEI in a ratio of 6:1 PEI:DNA (w/w) in PBS. The cells were transfected with a cDNA mixture consisting of: 0.143 μg GPCR, 0.286 μg Gα, 0.143 μg Gβ<sub>1</sub>-venus, 0.143 μg Gy<sub>2</sub>-venus, 0.143 μg masGRK3ct-Nluc and 0.143 μg Ric8A or Ric8B or pcDNA3.1.

The chaperone Ric8A was transfected together with Gα<sub>14</sub> and Gα<sub>15</sub> and Ric8B was transfected with Gα<sub>if</sub>.

For the cAMP BRET assays, where the toxins were exogenously added: The HEK293A ΔGα<sub>i/o</sub> CRISPR knockout cells were transfected using PEI in a ratio of 6:1 PEI:DNA (w/w) in PBS. The cells were transfected with a cDNA mixture consisting of: 0.143 μg D<sub>2</sub>R, 0.286 μg Gα<sub>2</sub>/Gα<sub>oA</sub>/Gα<sub>z</sub>/pcDNA3.1 and 0.429 μg CAMYEL sensor.

Assays, where the active A subunits of the toxins were transiently transfected, had the following conditions: HEK293T cells were transfected using PEI in a ratio of 1.5 PEI:1 DNA (w/w) mixed in 150 mM NaCl. For the G-protein activation assays the cells were transfected with 0.500 μg β<sub>1</sub>, 0.500 μg Venus-γ<sub>2</sub> and 0.100 μg masGRKctRluc8 as well as 1 μg of the G protein of interest together with 0.375 μg of a receptor suited for the specific G-protein class and 0.375 μg of the helper proteins Ric8A for Gα<sub>14</sub> and Gα<sub>15</sub> and Ric8B for Gα<sub>if</sub> and finally 0.200 μg of either the active subunit of PTX (PTX-S1), OZITX (OZITX-S1) or pcDNA3.1+ as a control. For the cAMP production inhibition assays the cells were co-transfected with 1 μg of the CAMYEL sensor (ATCC MBA-277). For the Ca<sup>2+</sup> assay, the cells were transfected with 0.3 μg of the receptor (M3R or D2LR), 0.3 μg of Gα<sub>q10/q13</sub> and 0.2 μg of either S1-PTX/S1-OZITX or pcDNA3.

**G-protein activation.** G-protein activation was measured using a BRET assay that monitors Gβγ release<sup>24,25</sup>. The HEK293A ΔGα-all cells were first transfected as described earlier and the following day the cells were harvested and transferred into white 96-well CulturPlates (PerkinElmer) in DMEM + 10% FBS. In the conditions where the cells were treated with OZITX or PTX, the cells were left to adhere before being treated in the 96-well plate 16–20 h before performing the assay. The G-protein activation assays were then performed ~24 h after plating out the transfected cells. The media in each well was aspirated, washed with Hank's balanced salt solution pH 7.4 (HBSS), replaced with HBSS and then kept at 37 °C for the remainder of the assay. Furimazine was added with a multi-stepper pipette 15 min before agonist addition and left to equilibrate. The agonist was then added, and cells were incubated in a LUMIstar Omega (BMG Labtech) plate reader. The BRET measurements were then taken 2.5 min after agonist addition. Simultaneous dual emission filters were used in the LUMIstar Omega for detection of the luciferase at 445–505 nm and venus at 505–565 nm, all measured at 37 °C. For G-protein activation assays where the toxin active A subunit cDNAs were transfected, the same protocol was followed with some exceptions: HEK293T cells were used instead of CRISPR/Cas gene-edited cells, DPBS + 5 mM glucose was used as the assay buffer, 96-well black-white isoplates were used, and the plate was detected five minutes after agonist stimulation in a PHERAstar FS (BMG Labtech). After acquiring the data, the ratio of the venus emission channel was then divided by the luciferase emission channel to determine the BRET ratio. The vehicle-subtracted raw BRET ratio (drug-induced increase in BRET) is plotted for the G-protein activation assay data.

**Gy-mVenus recruitment assay.** For the D<sub>2</sub>R-mediated Gy-mVenus recruitment assay, HEK293T cells were seeded onto six-well plates and transfected with a 1:6 ratio of DNA:polyethyleneimine with plasmids encoding D2R-nluc (50 ng), Gα<sub>oA/z</sub> WT (cDNA resource centre, Bloomsburg University, PA, 125 ng), human Gβ<sub>1</sub> (250 ng) and human Gy<sub>2</sub>-mVenus (250 ng). Cells were harvested from six-well plates 24 h after transfection and plated into poly-D-lysine coated (Sigma-Aldrich) white-bottom 96-well optiplates (Wallac, PerkinElmer Life and Analytical Sciences) at a density of 50,000 cells per well. Twenty-four hours after cells were transferred to plates, media was aspirated, cells washed once with DPBS and 80 μL DPBS containing 5 mM glucose was added to each well. In all, 10 μL of coelenterazine was added to each well and the plate read on the PHERAstar FS (BMG Labtech) for 5 min, paused for the addition of 10 μL agonists and read again for 10 min. After acquiring the data, the ratio of the venus emission channel was then divided by the luciferase emission channel to determine the BRET ratio. The vehicle-subtracted raw BRET ratio (drug-induced increase in BRET) is plotted for the G-protein recruitment assay data.

**Gα<sub>i/o/z</sub>-mediated inhibition of cAMP production.** The cAMP production inhibition assays' principle is based on the ability of a genetically encoded conformational BRET sensor to detect the relative concentrations of intracellular cAMP<sup>50</sup>. Initially, the transfected HEK293A ΔGα<sub>i/o</sub> cells were harvested and transferred into white 96-well CulturPlates in DMEM + 10% FBS 24 h after the transient transfection. When the cells were treated with OZITX or PTX, this occurred in the 96-well plate after adherence and about 18 h before the assay. Next, the cAMP inhibition assays were performed the following day after plating out the transfected cells and toxin or control treatment. On the day of the assay, the plate media was aspirated, washed once with HBSS pH 7.4 and replenished with HBSS pH 7.4 and then held at 37 °C for the rest of the experiment. In total, 5 μM coelenterazine-h was added 15 min before agonist addition. 10 μM Forskolin was added 10 min before agonist addition and the readings were then continuously taken in the live cells. Bioluminescence was detected on a LUMIstar Omega set to 37 °C. Simultaneous dual emission filters were used for the BRET donor at 445–505 nm and the acceptor at 505–565 nm. The ratio of the acceptor channel was then divided by the donor channel to determine the BRET ratio. The data was then

baseline-corrected to the vehicle control wells over time. A slightly modified protocol was followed for the assays where the active subunit cDNAs of the toxins were transfected: HEK293T cells were used instead of the HEK293A  $\Delta G\alpha_{i/o}$  cells, 96-well black-white isoplates were used, DPBS + 5 mM glucose was used as the assay buffer, a higher concentration of 30  $\mu$ M forskolin was used and this was co-added with the coelenterazine-h ten minutes prior to the addition of the agonist. The plate was then detected 20 min after agonist addition in a PHERAstar FS.

**Ca<sup>2+</sup> mobilisation assays.** Cells were seeded in a clear bottom black 96-well plate coated with poly-D-lysine (50  $\mu$ g/ml) at 100,000 cells per well. The following day, cells were washed with 100  $\mu$ l of 1 $\times$  HBSS assay buffer supplemented with 10 mM glucose, 4 mM probenecid at pH 7.4 and brilliant black, and then loaded with 100  $\mu$ l Fluo-4 AM (1  $\mu$ M) (prepared in DMSO and pluronic acid) for 45 min at 37 °C (no CO<sub>2</sub>). The release of Ca<sup>2+</sup> was measured using a Flexstation 3 (Molecular Devices; Sunnyvale, CA). Drug dilutions were prepared in assay buffer (without Fluo-4) at 6 $\times$  required concentration (volume 20  $\mu$ l in 100  $\mu$ l in Flexstation protocol) and transferred to a loading plate (transparent flat-bottom 96-well plate). Fluorescence was detected for 3 min 30 s at 485 nm excitation and 525 nm emission. Relative fluorescence units were normalised to the fluorescence stimulated by ionomycin to account for differences in cell number and loading efficiency.

**Data analysis, statistics and reproducibility.** GraphPad Prism 8 was used for data analysis and performing statistical tests. Statistical analysis was carried out with a Student's *t* test or one-way ANOVA followed by a post hoc test where appropriate. *P* values <0.05 were considered statistically significant. Data sets were of at least *n* = 3 and the experimental *n* number is stated for each data set in the corresponding figure legend. Figures depicting molecular structures were constructed using ICM-Browser (MolSoft LLC) and UCSF Chimera<sup>51</sup>. The covalent docking was carried out with the covDock module of Schrodinger suite (version 2021-1), assuming a SN2 nucleophilic substitution reaction, which results in the *a*-orientation of the attached ADP-ribose moiety on the asparagine<sup>52</sup>.

**Reporting summary.** Further information on research design is available in the Nature Research Reporting Summary linked to this article.

## Data availability

All original data have been deposited with *Communications Biology* in Supplementary Data 1 and are also available from the corresponding authors upon reasonable request.

## Materials availability

The cDNA for the S1 subunit of OZITX as described in the manuscript will be made available on reasonable request.

Received: 5 January 2021; Accepted: 17 February 2022;

Published online: 23 March 2022

## References

- Northup, J. K. et al. Purification of the regulatory component of adenylate cyclase. *Proc. Natl. Acad. Sci. USA* **77**, 6516–6520 (1980).
- Taylor, S. J., Smith, J. A. & Exton, J. H. Purification from bovine liver membranes of a guanine nucleotide-dependent activator of phosphoinositide-specific phospholipase C. Immunologic identification as a novel G-protein alpha subunit. *J. Biol. Chem.* **265**, 17150–17156 (1990).
- Hescheler, J., Rosenthal, W., Trautwein, W. & Schultz, G. The GTP-binding protein, Go9 regulates neuronal calcium channels. *Nature* **325**, 445 (1987).
- Hildebrandt, J. D. et al. Stimulation and inhibition of adenylyl cyclases mediated by distinct regulatory proteins. *Nature* **302**, 706 (1983).
- Buhl, A. M., Johnson, N. L., Dhanasekaran, N. & Johnson, G. L. Ga12 and Ga13 stimulate Rho-dependent stress fiber formation and focal adhesion assembly. *J. Biol. Chem.* **270**, 24631–24634 (1995).
- Sullivan, K. A. et al. Identification of receptor contact site involved in receptor–G protein coupling. *Nature* **330**, 758 (1987).
- Hamm, H. E. et al. Site of G protein binding to rhodopsin mapped with synthetic peptides from the alpha subunit. *Science* **241**, 832–835 (1988).
- Lee, E., Taussig, R. & Gilman, A. G. The G226A mutant of Gs alpha highlights the requirement for dissociation of G protein subunits. *J. Biol. Chem.* **267**, 1212–1218 (1992).
- Digby, G. J., Lober, R. M., Sethi, P. R. & Lambert, N. A. Some G protein heterotrimers physically dissociate in living cells. *Proc. Natl. Acad. Sci. USA* **103**, 17789–17794 (2006).
- Ng, N. M. et al. ExAB is a founding member of a new family of metalloprotease AB5 toxins with a hybrid cholera-like B subunit. *Structure* **21**, 2003–2013 (2013).
- Endo, Y. et al. Site of action of a Vero toxin (VT2) from *Escherichia coli* O157:H7 and of Shiga toxin on eukaryotic ribosomes: RNA N-glycosidase activity of the toxins. *Eur. J. Biochem.* **171**, 45–50 (1988).
- Katada, T. & Ui, M. Direct modification of the membrane adenylate cyclase system by islet-activating protein due to ADP-ribosylation of a membrane protein. *Proc. Natl. Acad. Sci. USA* **79**, 3129–3133 (1982).
- Cassel, D. & Pfeuffer, T. Mechanism of cholera toxin action: covalent modification of the guanyl nucleotide-binding protein of the adenylate cyclase system. *Proc. Natl. Acad. Sci. USA* **75**, 2669–2673 (1978).
- Orth, J. H. et al. Pasteurella multocida toxin activation of heterotrimeric G proteins by deamidation. *Proc. Natl. Acad. Sci. USA* **106**, 7179–7184 (2009).
- Katada, T. & Ui, M. ADP ribosylation of the specific membrane protein of C6 cells by islet-activating protein associated with modification of adenylate cyclase activity. *J. Biol. Chem.* **257**, 7210–7216 (1982).
- Casey, P. J., Fong, H. K., Simon, M. I. & Gilman, A. G. Gz, a guanine nucleotide-binding protein with unique biochemical properties. *J. Biol. Chem.* **265**, 2383–2390 (1990).
- Fong, H., Yoshimoto, K. K., Eversole-Cire, P. & Simon, M. I. Identification of a GTP-binding protein alpha subunit that lacks an apparent ADP-ribosylation site for pertussis toxin. *Proc. Natl. Acad. Sci. USA* **85**, 3066–3070 (1988).
- Matsuoka, M., Itoh, H., Kozasa, T. & Kaziro, Y. Sequence analysis of cDNA and genomic DNA for a putative pertussis toxin-insensitive guanine nucleotide-binding regulatory protein alpha subunit. *Proc. Natl. Acad. Sci. USA* **85**, 5384–5388 (1988).
- Kimple, M. E. et al. A role for Gz in pancreatic islet  $\beta$ -cell biology. *J. Biol. Chem.* **280**, 31708–31713 (2005).
- Kimple, M. E. et al. Gz negatively regulates insulin secretion and glucose clearance. *J. Biol. Chem.* **283**, 4560–4567 (2008).
- Brill, A. L. et al. Synergy between Gz deficiency and GLP-1 analog treatment in preserving functional  $\beta$ -cell mass in experimental diabetes. *Mol. Endocrinol.* **30**, 543–556 (2016).
- Fenske, R. J. et al. The inhibitory G protein  $\alpha$ -subunit, Gz, promotes type 1 diabetes-like pathophysiology in NOD mice. *Endocrinology* **158**, 1645–1658 (2017).
- Littler, D. R. et al. Structure–function analyses of a pertussis-like toxin from pathogenic *Escherichia coli* reveal a distinct mechanism of inhibition of trimeric G-proteins. *J. Biol. Chem.* **292**, 15143–15158 (2017).
- Hollins, B., Kuravi, S., Digby, G. J. & Lambert, N. A. The c-terminus of GRK3 indicates rapid dissociation of G protein heterotrimers. *Cell. Signal.* **21**, 1015–1021 (2009).
- Masuh, I., Martemyanov, K. A. & Lambert, N. A. in *G Protein-Coupled Receptors in Drug Discovery: Methods and Protocols* (ed. Marta, F.) 107–113 (Springer New York, 2015).
- Masuh, I., Xie, K. & Martemyanov, K. A. Macromolecular composition dictates receptor and G protein selectivity of regulator of G protein signaling (RGS) 7 and 9-2 protein complexes in living cells. *J. Biol. Chem.* **288**, 25129–25142 (2013).
- Hisano, Y. et al. Lysolipid receptor cross-talk regulates lymphatic endothelial junctions in lymph nodes. *J. Exp. Med.* **216**, 1582–1598 (2019).
- Lane, J. R., Powney, B., Wise, A., Rees, S. & Milligan, G. G protein coupling and ligand selectivity of the D2L and D3 dopamine receptors. *J. Pharmacol. Exp. Therapeutics* **325**, 319–330 (2008).
- Donthamsetti, P. et al. Arrestin recruitment to dopamine D2 receptor mediates locomotion but not incentive motivation. *Mol. Psychiatry* **25**, 2086–2100 (2018).
- Eden, R. et al. Preclinical pharmacology of ropinirole (SK&F 101468-A) a novel dopamine D2 agonist. *Pharmacol. Biochem. Behav.* **38**, 147–154 (1991).
- Dearry, A. et al. Molecular cloning and expression of the gene for a human D1 dopamine receptor. *Nature* **347**, 72 (1990).
- Zhou, Q.-Y. et al. Cloning and expression of human and rat D1 dopamine receptors. *Nature* **347**, 76 (1990).
- Seeman, P. & Niznik, H. Dopamine D1 receptor pharmacology. *ISI Atlas Sci. Pharm.* **2**, 161–170 (1988).
- Andersen, P. H. & Jansen, J. A. Dopamine receptor agonists: selectivity and dopamine D1 receptor efficacy. *Eur. J. Pharmacol.: Mol. Pharmacol.* **188**, 335–347 (1990).
- Wu, T., Li, A. & Wang, H.-L. Neurotensin increases the cationic conductance of rat substantia nigra dopaminergic neurons through the inositol 1, 4, 5-trisphosphate-calcium pathway. *Brain Res.* **683**, 242–250 (1995).
- Wang, H.-L. & Wu, T. Gαq11 mediates neurotensin excitation of substantia nigra dopaminergic neurons. *Mol. Brain Res.* **36**, 29–36 (1996).
- Besserer-Offroy, É. et al. The signaling signature of the neurotensin type 1 receptor with endogenous ligands. *Eur. J. Pharmacol.* **805**, 1–13 (2017).
- Hildebrandt, J., Hanoune, J. & Birnbaumer, L. Guanine nucleotide inhibition of cyc-S49 mouse lymphoma cell membrane adenylyl cyclase. *J. Biol. Chem.* **257**, 14723–14725 (1982).
- Vivaudou, M. et al. Probing the G-protein regulation of GIRK1 and GIRK4, the two subunits of the KACH channel, using functional homomeric mutants. *J. Biol. Chem.* **272**, 31553–31560 (1997).

40. Castro, M. G., McNamara, U. & Carbonetti, N. H. Expression, activity and cytotoxicity of pertussis toxin S1 subunit in transfected mammalian cells. *Cell. Microbiol.* **3**, 45–54 (2001).
41. Senogles, S. E. The D2 dopamine receptor isoforms signal through distinct G $\alpha$  proteins to inhibit adenylyl cyclase. A study with site-directed mutant G $\alpha$  proteins. *J. Biol. Chem.* **269**, 23120–23127 (1994).
42. Joshi, S. A., Fan, K. P., Ho, V. W. & Wong, Y. H. Chimeric G $\alpha$ q mutants harboring the last five carboxy-terminal residues of G $\alpha$ i2 or G $\alpha$ o are resistant to pertussis toxin-catalyzed ADP-ribosylation. *FEBS Lett.* **441**, 67–70 (1998).
43. Reisine, T. Pertussis toxin in the analysis of receptor mechanisms. *Biochemical Pharmacol.* **39**, 1499–1504 (1990).
44. Doi, M. et al. Gpr176 is a Gz-linked orphan G-protein-coupled receptor that sets the pace of circadian behaviour. *Nat. Commun.* **7**, 10583 (2016).
45. Gonzalez-Iglesias, A. E., Murano, T., Li, S., Tomić, M. & Stojilkovic, S. S. Dopamine inhibits basal prolactin release in pituitary lactotrophs through pertussis toxin-sensitive and -insensitive signaling pathways. *Endocrinology* **149**, 1470–1479 (2007).
46. van den Buuse, M. et al. Enhanced effect of dopaminergic stimulation on prepulse inhibition in mice deficient in the alpha subunit of Gz. *Psychopharmacology* **183**, 358–367 (2005).
47. Bahia, D. S. et al. Hydrophobicity of residue351 of the G protein G $\alpha$ i4 determines the extent of activation by the  $\alpha$ 2A-adrenoceptor. *Biochemistry* **37**, 11555–11562 (1998).
48. Kim, K. et al. Structure of a hallucinogen-activated Gq-coupled 5-HT2A serotonin receptor. *Cell* **182**, 1574–1588 (2020).
49. Zhuang et al. Structural insights into the human D1 and D2 dopamine receptor signaling complexes. *Cell* **184**, 931–942 (2021).
50. Jiang, L. I. et al. Use of a cAMP BRET sensor to characterize a novel regulation of cAMP by the sphingosine 1-phosphate/G13 pathway. *J. Biol. Chem.* **282**, 10576–10584 (2007).
51. Pettersen, E. F. et al. UCSF Chimera—a visualization system for exploratory research and analysis. *J. Comput. Chem.* **25**, 1605–1612 (2004).
52. Sung, V. M. “Mechanistic overview of ADP-ribosylation reactions.”. *Biochimie* **113**, 35–46 (2015).

## Acknowledgements

This work was supported by the National Health and Medical Research Council (NHMRC, Australia, Project Grant 1049564), a Schaefer Research Scholars Program Award (Columbia University, New York, USA) and the Biotechnology and Biological Sciences Research Council (BB/T013966/1) to J.R.L. and National Institute of Health (NIH) grant MH54137 to J.A.J.

## Author contributions

A.C.K., M.H.P., J.A.J. and J.R.L. designed experiments. A.C.K., M.H.P. and L.L. performed experiments. A.C.K., M.H.P., L.L., J.A.J. and J.R.L. analysed the data. A.C.K., M.H.P., L.L., L.S., J.A.J., M.C. and J.R.L. wrote the manuscript. D.R.L., Y.O., T.B., A.I. and D.J.S. provided reagents.

## Competing interests

The authors declare no competing interests.

## Additional information

**Supplementary information** The online version contains supplementary material available at <https://doi.org/10.1038/s42003-022-03191-5>.

**Correspondence** and requests for materials should be addressed to Jonathan A. Javitch or J. Robert Lane.

**Peer review information** *Communications Biology* thanks Ka Young Chung and the other, anonymous, reviewers for their contribution to the peer review of this work. Primary Handling Editors: Nicolas Fanget and Karli Montague-Cardoso. Peer reviewer reports are available.

**Reprints and permission information** is available at <http://www.nature.com/reprints>

**Publisher's note** Springer Nature remains neutral with regard to jurisdictional claims in published maps and institutional affiliations.



**Open Access** This article is licensed under a Creative Commons Attribution 4.0 International License, which permits use, sharing, adaptation, distribution and reproduction in any medium or format, as long as you give appropriate credit to the original author(s) and the source, provide a link to the Creative Commons license, and indicate if changes were made. The images or other third party material in this article are included in the article's Creative Commons license, unless indicated otherwise in a credit line to the material. If material is not included in the article's Creative Commons license and your intended use is not permitted by statutory regulation or exceeds the permitted use, you will need to obtain permission directly from the copyright holder. To view a copy of this license, visit <http://creativecommons.org/licenses/by/4.0/>.

© The Author(s) 2022